Raman scattering in quantum wells in a high magnetic field: Fröhlich interaction

A. Cros
Departamento de Física Aplicada, Universidad de Valencia, Burjasot, E-46100 Valencia, Spain

A. Cantarero,* C. Trallero-Giner,† and M. Cardona
Max-Planck-Institut für Festkörperforschung, Heisenbergstrasse 1, Postfach 80 05 65, D-7000 Stuttgart 80, Federal Republic of Germany

(Received 27 February 1992; revised manuscript received 24 July 1992)

An explicit expression for the Raman-scattering efficiency in quantum wells (QW's) under high magnetic fields is given for the allowed Fröhlich electron-phonon interaction mechanism. The basic features of the theory are studied with a parabolic band approximation, which allows us to understand the physics involved in the selection rules and the double resonance conditions. Furthermore, a Luttinger Hamiltonian is used to describe the heavy-hole–light-hole admixture in III-V compounds. Selection rules are derived for backscattering configuration and circular polarizations. Phonons can couple via Fröhlich interaction with either light or heavy components of a QW subband, and both intrasubband and intersubband scattering become possible, the selection rule being $\Delta N = 0$ for the Landau quantum number. The phonon confinement is studied in thin QW's and a comparison among the different phonon modes is presented: only even phonon modes couple via Fröhlich interaction for $q_\perp = 0$. We have calculated the Raman polarizability of a 100-Å GaAs/AlAs multiple quantum well and compared it with recent experimental results.

I. INTRODUCTION

Resonant magneto-Raman scattering has become one of the most suitable techniques for the investigation of nonparabolicities and valence-band mixing in III-V semiconductor compounds, quantum wells, and superlattices.[1–7] It has the advantage over other interband magneto-optic techniques that we can go further in energy without loss of sensitivity, because the Raman process becomes resonant whenever the laser or scattered energy corresponds to an electronic transition between Landau levels (incoming or outgoing resonances, respectively). Backscattering geometry only needs thicknesses of about 1000 Å. In the case of quantum wells (QW's) and superlattices (SL's) the reduction in the dimensionality lifts the valence-band degeneracy of the bulk, and the information contained in the Raman spectra increases. With the application of an external magnetic field the energy spectrum quantizes completely, leading to the zero-dimensional quantization responsible for the well-known quantum Hall effect.[8]

When the energy difference between incoming and outgoing resonances corresponds to a phonon energy, there is a strong enhancement of the Raman intensity because the process becomes doubly resonant (DRRS). These double resonances have been achieved by applying stress,[9] varying the magnetic field,[5] or changing the thickness of a SL.[10] In recent magneto-Raman measurements on a 100-Å GaAs/AlAs multiple-QW structure, Calle *et al.*[6,7] have obtained a huge increase in the Raman intensity at a particular magnetic field, which has been related to an exciton-band double-resonant transition.

Theoretical and experimental studies of magneto-Raman scattering have been performed in recent years. Ruf *et al.*[2–4] investigated the Raman spectra of InP and GaAs under high magnetic fields. Trallero-Giner, Ruf, and Cardona[11] developed a theoretical model of one-phonon resonant Raman scattering under high magnetic fields, which explained satisfactorily the above magneto-Raman results. This model was extended[5] by taking into account the valence-band mixing through a Luttinger-type Hamiltonian.[12] The theory of magneto-Raman scattering in diluted magnetic semiconductors was developed by Limmer *et al.*[13] taking excitonic states as intermediate states in the process and that theory was compared with experimental results for $Cd_xMn_{1-x}Te$. Also some attention has been paid to the experimental[14] and theoretical[15] study of multiphonon Raman scattering in magnetic fields.

There are only a few theoretical studies of Raman scattering by phonons in QW's. Huang *et al.* worked out a detailed microscopic theory of Raman scattering in QW's based on the Luttinger Hamiltonian.[16] Cros *et al.*[17] developed a model theory of one-phonon resonant Raman scattering in high magnetic fields using for the electron-phonon interaction the bulk deformation-potential Hamiltonian. In the present work we study the Raman scattering induced by the Fröhlich interaction in QW's in an external magnetic field, which requires taking explicitly into account the confinement of the phonon modes.

The paper is organized as follows. In Sec. II the Raman polarizability induced by Fröhlich interaction is derived, and the resulting scattering efficiency is discussed in the context of a three-band parabolic model. In Sec. III the previous model is extended to take into account the complexity of the semiconductor band structure using a 4×4 Luttinger Hamiltonian. In Sec. IV the previous calcula-

tions are compared with experimental results carried on a 100-Å GaAs/AlAs multiple QW in a magnetic field while Sec. V summarizes the main conclusions of the work.

II. THEORETICAL MODEL OF ONE-PHONON RESONANT RAMAN SCATTERING IN A SEMICONDUCTOR QW

Raman intensities are usually given in terms of the scattering efficiency $dS/d\Omega$ or, equivalently, the Raman polarizability a.[18] Within a microscopic theory, the Raman polarizability is directly proportional to the probability amplitude W_{FI} between an initial state $|I\rangle$ and a final state $|F\rangle$.[18,19] Resonant Raman scattering can be treated as a third-order process in perturbation theory; thus, two electron-photon interactions and one electron-phonon interaction terms appear in the amplitude probability. Explicit expressions for these interaction Hamiltonians are given, for instance, in Ref. 17. There, the deformation-potential electron-phonon interaction was studied, while here, our purpose is to study the case of Fröhlich interaction.

The Fröhlich electron-phonon interaction Hamiltonian has been derived for a single QW in Ref. 20. It is based on a continuum model for the long-wavelength polar-optical phonons assuming them to be dispersive and completely confined to the QW. The vibrational amplitude used in the derivation of the Fröhlich Hamiltonian has been shown to satisfy simultaneously mechanical and electrostatic boundary conditions.[21] Within this model the electrostatic potential derived from the polarization field by the usual procedure gives for the coupling constant $S_\mu^\beta(\mathbf{q})$ the following expression:[20]

$$S_\mu^\beta(\mathbf{q}) = \frac{1}{\sqrt{V}}\sqrt{\frac{\omega_{\rm LO}}{\omega_q}}\frac{C_F^*}{|\mathbf{q}|}\langle\mu \mid \Phi_{\mathbf{q}}^*(z_e)\exp(-i\mathbf{q}_\perp\cdot\boldsymbol{\rho}_e) - \Phi_{\mathbf{q}}^*(z_h)\exp(-i\mathbf{q}_\perp\cdot\boldsymbol{\rho}_h)|\beta\rangle, \tag{1}$$

where C_F is the Fröhlich constant,

$$C_F = -i\sqrt{2\pi e^2\hbar\omega_{\rm LO}\left(\frac{1}{\varepsilon_\infty}-\frac{1}{\varepsilon_0}\right)}\,, \tag{2}$$

ε_0 and ε_∞ are the static and optical dielectric constants, and $\omega_q^2 = \omega_{\rm LO}^2 - \mu^2 q_z^2$ represents the dispersion of the LO-phonon frequency, μ being a constant to be determined by fitting the experimental phonon-dispersion relations, $\boldsymbol{\rho}$ and $\mathbf{q}_\perp$ are the components of space coordinate and momentum in the plane of the layers, and $V = L^2 d$ the volume of the QW. In Eq. (1) the modulation function $\Phi_{\mathbf{q}}(z)$ takes into account the confinement of the phonon in the quantum well.[20] The quantity q_z is quantized, $q_z = p\pi/d$, where $p = 1, 2, 3...$ is a positive integer whose value is limited by the condition that q_z must stay within the first Brillouin zone of the bulk crystal.

We proceed in a similar way to that in Ref. 17. As a first step we discuss the physics of the problem through a simplified model involving the substitution of the Luttinger Hamiltonian by a Hamiltonian with Landé factors for the holes.

A. Wave functions and matrix elements

We take the z axis as the growth direction, the magnetic field also along z, and choose the Landau gauge for the vector potential ($\nabla\cdot\mathbf{A} = 0$), with $\mathbf{A} = B\,(0, x, 0)$.

The Schrödinger equation can be separated into three differential equations, and the normalized wave function is obtained:[17]

$$\Psi_{Nl} = \frac{1}{\sqrt{L}}e^{ik_y y}\varphi_l(z)u_N(x-x_0)v_0(\mathbf{r})\,, \tag{3}$$

where $u_N(x-x_0)$ is the wave function of the one-dimensional harmonic oscillator, centered at $x_0 = -\frac{\hbar}{eB}k_y \equiv -R^2 k_y$, with Landau number N and $\varphi_l(z)$ is the wave function corresponding to the QW potential. The envelope function has been multiplied by the corresponding Bloch function $v_0(\mathbf{r})$ calculated at $\mathbf{k} = 0$. The energy of the system is given by

$$E = \hbar\omega_c(N+\tfrac{1}{2}) + E_l + g m_s \mu_B B, \tag{4}$$

where $m_s = \pm\frac{1}{2}$ for the two spin states, and E_l are the energies of electrons and holes in the QW potential.

Using the set of wave functions of Eq. (3) we can calculate the matrix elements that appear in the amplitude probability. For electron-radiation interaction we have[17]

$$\langle\beta|H_{ER}|I\rangle = \frac{e}{m_0}\sqrt{\frac{h}{V\omega_l\eta_l^2}}G_{l_e,l_h}\delta_{N_e,N_h}\delta_{k_{ye},k_{yh}+\kappa_y}\,, \tag{5}$$

$$\langle F|H_{ER}|\mu\rangle = \frac{e}{m_0}\sqrt{\frac{h}{V\omega_s\eta_s^2}}G^*_{l_e,l_h}\delta_{N_e,N_h}\delta_{k_{ye},k_{yh}-\kappa_y}\,, \tag{6}$$

where the functions G_{l_1,l_2} are proportional to the overlap integrals of the well functions:[22]

$$G_{l_1,l_2} = \mathbf{e}\cdot\mathbf{p}_{cv}\int_{-\infty}^{+\infty}\varphi^*_{l_1}(z)\,\varphi_{l_2}(z)\,dz \tag{7}$$

and $\mathbf{p}_{cv}$ is the momentum matrix element between the valence and conduction bands. ω is the photon frequency and η the refractive index, the indices l and s refer to laser and scattered light, respectively, κ is the photon wave vector, and m_0 is the free-electron mass. The indices l (laser light) and s (scattered light) have been omitted in G_{l_1,l_2}. The matrix elements corresponding to the electron- and hole-lattice interactions are

$$\langle\mu|H_{EP}|\beta\rangle = \frac{1}{\sqrt{V}}\sqrt{\frac{\omega_{\rm LO}}{\omega_q}}\frac{C_F^*}{q}\{F_{l'_e,l_e}f^e_{N'_e,N_e}e^{-iq_x x_{o,e}}\delta_{N'_h,N_h}\delta_{k'_{yh},k_{yh}+q_y}\delta_{l'_h,l_h} - F_{l'_h,l_h}f^h_{N'_h,N_h}e^{-iq_x x_{o,h}}\delta_{N'_e,N_e}\delta_{k'_{ye},k_{ye}+q_y}\delta_{l'_e,l_e}\}\delta_{v',v}\delta_{c',c}\,, \tag{8}$$

where the functions F_{l_1,l_2} and $f^{\alpha}_{N_1,N_2}$ represent

$$F_{l_1,l_2}(q) = \int_{-\infty}^{+\infty} \varphi^*_{l_1}(z)\varphi_{l_2}(z)\Phi^*_q(z)\,dz, \tag{9}$$

$$f^{h}_{N_1,N_2}(q_x,q_y) = f^{e}_{N_1,N_2}(q_x,-q_y) = \int_{-\infty}^{+\infty} u^*_{N_1}(x)u_{N_2}(x+q_yR^2)e^{-iq_xx}\,dx. \tag{10}$$

The fact that the Fröhlich Hamiltonian does not act on the Bloch part of the wave functions is implicit in Eq. (8). The processes will be purely intraband as in the bulk case. In the following we will omit the $\delta_{c',c}$ and $\delta_{v',v}$ for simplicity.

Taking the wave vectors of the laser and scattered light, $\kappa_l \sim \kappa_s \sim 0$, and calculating the sum in $k_{yh(e)}$,

$$\sum_{k_{yh(e)}} e^{-iq_xx_{0,h(e)}} = \frac{L^2}{2\pi R^2}\delta_{q_x,0}\ . \tag{11}$$

The probability amplitude can be written as

$$W_{FI} = \frac{K_{ls}}{q\sqrt{\omega_q}} \sum_{N,m_s} \sum_{l_e,l'_e} \sum_{l_h,l'_h} G^*_{l'_e,l'_h} G_{l_e,l_h} \frac{\delta_{l'_h,l_h}F_{l'_e,l_e}(\mathbf{q}) - \delta_{l'_e,l_e}F_{l'_h,l_h}(\mathbf{q})}{(\hbar\omega_s - E_\mu + i\Gamma_\mu)(\hbar\omega_l - E_\beta + i\Gamma_\beta)} \tag{12}$$

with

$$K_{ls} = \frac{e^3BC^*_F\sqrt{\omega_{\mathrm{LO}}}}{\sqrt{V}m_0^2\eta_l\eta_s\sqrt{\omega_l\omega_s}d}\ . \tag{13}$$

The energy of the intermediate states is

$$\begin{aligned} E_{\beta(\mu)} = {} & E_g(c(c'),v(v')) + E_{l_h(l'_h)} \\ & + E_{l_e(l'_e)} + \hbar\bar{\omega}_c(\bar{\omega}_{c'})(N+\tfrac{1}{2}) \\ & + \mu_B m_s B(g_{e(e')} + g_{h(h')}), \end{aligned} \tag{14}$$

$\bar{\omega}_c$ being the cyclotron frequency with the reduced mass $\bar{m}$ ($\bar{m}^{-1} = m^{-1}_{e\perp} + m^{-1}_{h\perp}$), and $E_g(c,v)$ the energy gap between the valence and conduction states involved in the Raman process. According to Eqs. (12) and (14) the incoming and outgoing resonances will occur at frequencies

$$\begin{aligned} \hbar\omega_{l(s)}(l_e,l_h,N) = {} & E_g + E_{l_e} + E_{l_h} + \hbar\bar{\omega}_c(N+\tfrac{1}{2}) \\ & + \mu_B m_s(g_e+g_h)B. \end{aligned} \tag{15}$$

B. Selection rules

We will consider a QW grown in the (001) direction of a cubic semiconductor crystal in the Faraday configuration ($\mathbf{B} \parallel \boldsymbol{\kappa}_l \parallel z$), and derive the selection rules for backscattering geometry. The polarization of the light is referred to the fixed z axis, with right (+) and left (−) polarized light corresponding, respectively, to $\mathbf{e}_+ = (\mathbf{e}_x + i\mathbf{e}_y)/\sqrt{2}$, $\mathbf{e}_- = (\mathbf{e}_x - i\mathbf{e}_y)/\sqrt{2}$ polarization vectors.

Owing to wave-vector conservation, the optical phonons excited in the backscattering process propagate parallel to the z direction. Furthermore, the function $\Phi_{\mathbf{q}}(z)$ (Refs. 20 and 21) has a definite parity with respect to the bisector plane of the well, being even for even modes ($p = 2,4,6\ldots$) and odd for odd modes ($p = 1,3,5\ldots$): For $p = 2,4,6\ldots$

$$\Phi_{\mathbf{q}} \equiv \Phi_p(z) = \begin{cases} 0, & z < -d/2 \\ 2[(-1)^{\frac{p}{2}}\cos\frac{p\pi}{d}z - 1], & -d/2 < z < d/2 \\ 0, & z > d/2. \end{cases} \tag{16}$$

If $p = 1,3,5\ldots$ we have

$$\Phi_{\mathbf{q}} \equiv \Phi_p(z) = \begin{cases} 2, & z < -d/2 \\ 2(-1)^{\frac{p+1}{2}}\sin\frac{p\pi}{d}z, & -d/2 < z < d/2 \\ -2, & z > d/2. \end{cases} \tag{17}$$

Equation (8) shows that when the electron is scattered, the hole remains in the same subband. That means that both electron subbands must have the same parity, in order for $G_{l'_e,l_h}$ and G_{l_e,l_h} not to vanish. If the electron subbands l'_e and l_e have the same parity, the function $\Phi_p(z)$ must be even. In that case $F_{l'_e,l_e}$ is different from zero. Odd modes are thus forbidden for Fröhlich interaction. We can conclude then that only even confined phonon modes are excited in the Raman process under consideration.

Once we know the condition for $F_{l',l}$ to be nonzero, the selection rules for the optical transitions are derived from the momentum matrix elements to be the same as in bulk materials, with the additional possibility of intersubband transitions. The only nonzero matrix elements are[23]

$$\begin{aligned} & \langle c\uparrow|\mathbf{e}_-\cdot\mathbf{p}|v^+_{\mathrm{hh}}\rangle = \langle c\downarrow|\mathbf{e}_+\cdot\mathbf{p}|v^-_{\mathrm{hh}}\rangle = iP, \\ & \langle c\uparrow|\mathbf{e}_+\cdot\mathbf{p}|v^-_{\mathrm{lh}}\rangle = \langle c\downarrow|\mathbf{e}_-\cdot\mathbf{p}|v^+_{\mathrm{lh}}\rangle = \frac{i}{\sqrt{3}}P, \\ & \langle c\uparrow|\mathbf{e}_+\cdot\mathbf{p}|v^-_{\mathrm{so}}\rangle = \langle c\downarrow|\mathbf{e}_-\cdot\mathbf{p}|v^+_{\mathrm{so}}\rangle = -i\sqrt{\tfrac{2}{3}}P, \end{aligned} \tag{18}$$

where $P = \langle x|p_x|c\rangle$, and the selection rules for backscattering and circularly polarized light are

$\bar{z}(\sigma^-,\sigma^-)z$	$\bar{z}(\sigma^+,\sigma^+)z$
$v^+_{hh} \rightarrow v^+_{hh}(\uparrow)$	$v^-_{hh} \rightarrow v^-_{hh}(\downarrow)$
$v^+_{lh} \rightarrow v^+_{lh}(\downarrow)$	$v^-_{lh} \rightarrow v^-_{lh}(\uparrow)$
$v^+_{so} \rightarrow v^+_{so}(\downarrow)$	$v^-_{so} \rightarrow v^-_{so}(\uparrow)$

(19)

The couplings mediated by the Fröhlich interaction conserve the Landau number, $\Delta N = 0$, the third component of the angular momentum, $\Delta J_z = 0$, and the spin ($\Delta m_s = 0$). In the crossed configuration $[\bar{z}(\sigma^\pm,\sigma^\mp)z]$ the Raman efficiency is zero.

C. Raman efficiency within the simplified model

In order to obtain the Raman-scattering efficiency $dS/d\Omega$, we need to calculate the Raman polarizability corresponding to one phonon mode and add over all phonon modes with the restriction $\omega_q^2 > 0$. The resulting final expression can be written as

$$\frac{dS}{d\Omega} = S_0 \sum_{p \text{ even}} \frac{1}{p^2 \omega_q} \left| \sum_{N,m_s} \sum_{l'_e,l_e} \sum_{l'_h,l_h} \frac{G^*_{l'_e,l'_h} G_{l_e,l_h} \left[\delta_{l'_h,l_h} F_{l'_e,l_e} - \delta_{l'_e,l_e} F_{l'_h,l_h}\right]}{(\hbar\omega_s - E_\mu + i\Gamma_\mu)(\hbar\omega_l - E_\beta + i\Gamma_\beta)} \right|^2 , \tag{20}$$

where the constant S_0 is

$$S_0 = \frac{\omega_s^2 \eta_s e^6 B^2 |C_F|^2 \omega_{LO}}{\omega_l^2 \eta_l \pi^4 \hbar^2 c^4 m_0^4} . \tag{21}$$

In thin QW's ($d \lesssim 50$ Å) the different phonon modes are going to have well-defined, different frequencies because of the bulk dispersion. In that case, the $dS/d\Omega$ must be calculated for a fixed p. For quantum wells wide enough ($d \gtrsim 50$ Å) so that the separation between individual confined modes is less than their width, the nondispersive approximation can be made, setting $\omega_q = \omega_{LO}$ and adding all the efficiencies corresponding to the different phonon modes in order to obtain the total Raman efficiency. The number of phonon modes we need to add is not high because of the factor p^2 that appears in Eq. (20).

We have calculated the scattering cross section $dS/d\Omega$ within this model for QW's of different thicknesses as a function of laser frequency for the scattering configuration $\bar{z}(\sigma^+,\sigma^+)z$, whose selection rules are given in Eq. (19). For this purpose we first calculated the energy subbands (including the QW confined electronic sublevels and their masses in a self-consistent way) and the corresponding well wave-functions $\varphi_l(z)$ ($l = l_e, l_{lh}, l_{hh}$) as explained in Ref. 17. The matrix elements were then evaluated with the wave functions of Eq. (3), and the scattering efficiency was finally obtained by means of Eq. (20). The parameters used in the calculations are those for GaAs/AlAs QW's, given in Table I. The lifetimes used for the calculation of $dS/d\Omega$ were taken from a least-squares fit to a photoluminescence excitation profile.[6] They are assumed to increase quadratically with the Landau number N. The numerical expression used is

$$\Gamma(N) = 1.2 - 0.47(N+1) + 0.26(N+1)^2 \tag{22}$$

independently of the light or heavy character of the band.

In Fig. 1 we show the scattering efficiency as a function of laser energy for 135-, 145-, and 150-Å QW's in the $\bar{z}(\sigma^+,\sigma^+)z$ configuration with the magnetic field kept fixed at 8 T. The selection rules given in Eq. (19) show that only states of the same valence band and the same parity are coupled by the Fröhlich interaction. The peaks in the spectra correspond to intrasubband transitions. For $d = 145$ Å the energy difference between the first and third heavy-hole well states equals that of the

TABLE I. Parameters used to calculate the Landau levels in GaAs/AlAs QW's. For the band offset the ratio 68/32 has been used.

Parameters	Values	Reference
E_g(GaAs)	1520 meV	25
E_g(AlAs)	2766 meV	25
P	0.65 a.u.	a
m_{hh}(GaAs)	$0.34m_0$	25
m_{hh}(AlAs)	$0.55m_0$	25
ω_{LO}	36 meV	26
g_e	−0.44	27
$g_{3/2}$	7.2	17
$g_{1/2}$	−2.4	17

[a] $P \approx \frac{2\pi}{a}$.

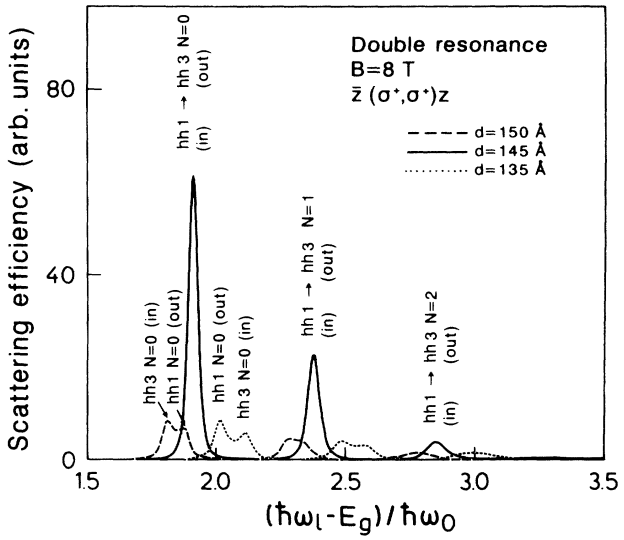

FIG. 1. Calculated Raman-scattering efficiency, according to Eq. (20), in the $\bar{z}(\sigma^+,\sigma^+)z$ configuration close to a double resonance. The magnetic field has been kept at 8 T. The parameters of Table I have been used.

phonon. Because the Fröhlich interaction couples these two QW levels, a double resonance for the hh3→ hh1 transition is obtained at a laser energy $E_g+1.94\hbar\omega_{\rm LO}$. In the parabolic QW model, energy levels of the same subband depend linearly on the magnetic field with the same slope for levels with the same Landau number, so that the double resonance condition is independent of magnetic field. This condition is fulfilled simultaneously for the different Landau levels of the bands involved in the transition. In Fig. 1 we can see the double resonant peaks corresponding to Landau levels N=0, 1, and 2 [labeled as (in)(out)]. The difference in intensity is due to the dependence of the linewidth on Landau quantum number. When we change the well thickness, the splitting between hh1 and hh3 changes and the double resonance is lost as the incoming and outgoing resonances separate. The energy at which the resonances appear depends linearly on the magnetic field:

$$\hbar\omega_l = E_g + E_{l_e} + E_{l_h} + \hbar eB\left(\frac{1}{m_{e_\perp}} + \frac{1}{m_{h_\perp}}\right)(N+\tfrac{1}{2}) + \mu_B(g_e+g_h)m_{se}B. \quad (23)$$

III. MIXING EFFECTS

We derive next the Raman efficiency taking the coupling of the different energy bands into account. For a QW grown in the (001) direction, and using the 4×4 Luttinger Hamiltonian[24] (we assume a very large spin-orbit splitting), we determine the weight coefficients which characterize the field-dependent mixing of the bands ($C_{l_i}^{\alpha,n}$). As a result of the coupling, the wave functions are given by[25]

$$\Psi_{\alpha,n} = \frac{1}{\sqrt{L}}\begin{pmatrix}\phi_1^{\alpha n}(z)u_{n-3}(x-x_0)v_1\\ \phi_2^{\alpha n}(z)u_{n-2}(x-x_0)v_2\\ \phi_3^{\alpha n}(z)u_{n-1}(x-x_0)v_3\\ \phi_4^{\alpha n}(z)u_n(x-x_0)v_4\end{pmatrix}e^{ik_y y}. \quad (24)$$

Here $v_1 = v_{\rm hh}^+ = \left|\frac{3}{2},+\frac{3}{2}\right\rangle$, $v_2 = v_{\rm lh}^+ = \left|\frac{3}{2},+\frac{1}{2}\right\rangle$, $v_3 = v_{\rm lh}^- = \left|\frac{3}{2},-\frac{1}{2}\right\rangle$, and $v_4 = v_{\rm hh}^- = \left|\frac{3}{2},-\frac{3}{2}\right\rangle$; $u_n \equiv 0$ if $n<0$, n being the oscillator number. The function $\phi_i^{\alpha,n}(z)$ is a linear combination of the QW functions $\varphi_{li}(z)$:

$$\phi_i^{\alpha,n}(z) = \sum_{l_i} C_{l_i}^{\alpha,n}\varphi_{l_i}(z). \quad (25)$$

The index α is the new quantum number derived from the diagonalization of the well Hamiltonian in the presence of the magnetic field. The mixing increases with increasing magnetic field and Landau-level index.

A. Scattering efficiency and selection rules

We derive the scattering amplitude from the wave functions (24). The probability amplitude is found to be

$$W_{FI} = \frac{K_{ls}}{q\sqrt{\omega_q}}\sum_{N,m_s}\sum_{l_e,l'_e}\sum_{\alpha,\alpha'} G^*_{l'_e,\alpha'}G_{l_e,\alpha}\frac{\delta_{\alpha',\alpha}F_{l'_e,l_e}(q_z)-\delta_{l'_e,l_e}F_{\alpha',\alpha}(q_z)}{(\hbar\omega_s - E_\mu + i\Gamma_\mu)(\hbar\omega_l - E_\beta + i\Gamma_\beta)}, \quad (26)$$

with the following definitions:

$$G_{l_e,\alpha} = \sum_n\sum_{i=1}^4 \delta_{n-4+i,N}\,\mathbf{e}\cdot\mathbf{p}_{cv_i}\int \varphi_{l_e}(z)^*\phi_i^{\alpha,n}\,dz, \quad (27)$$

$$F_{\alpha',\alpha} = \sum_n\sum_{i=1}^4 \delta_{n-4+i,N}\int \phi_i^{\alpha',n\,*}(z)\phi_i^{\alpha,n}(z)\Phi_q^*(z)\,dz. \quad (28)$$

The energies of the intermediate states are now

$$E_{\beta(\mu)} = E_g(c(c'),v(v')) + E_{\alpha(\alpha')} + E_{l_e(l'_e)} + \hbar\omega_c(\omega_{c'})(N+\tfrac{1}{2}) + \mu_B m_s B g_{e(e')}. \quad (29)$$

In Eqs. (27) and (28), for a particular value of the spin m_s and polarization $\mathbf{e}$, i is fixed [see Eq. (19)], n is then fixed by the δ function, and the expressions reduce to

$$G_{l_e,\alpha} = \sum_{l_i} C_{l_i}^{\alpha,N+4-i}G_{l_e,l_i}, \quad (30)$$

$$F_{\alpha',\alpha} = \sum_{l_i}\sum_{l_j} C_{l_i}^{\alpha',N+4-i\,*}C_{l_j}^{\alpha,N+4-i}F_{l_i,l_j}. \quad (31)$$

The transitions mediated by the Fröhlich interaction are only possible with polarizations $\bar{z}(\sigma^+,\sigma^+)z$ and $\bar{z}(\sigma^-,\sigma^-)z$. In both configurations, the coupled levels are such that $\Delta n = \Delta N = 0$. As before, only intraband coupling is allowed.

B. Raman scattering in GaAs/AlAs QW's

The simplest, unambiguous way to label the hole Landau levels is by means of (n,α), the Landau oscillator quantum number, and a new quantum number α arising from the diagonalization of the Hamiltonian. Unfortunately, this labeling does not explicitly display the physical information that it actually contains. We know that deformation-potential interaction is interband and couples light- and heavy-hole states while Fröhlich interaction is intraband and couples either light-light or heavy-heavy states; this restricts the Landau sublevels involved in the process.

For $B=0$ ($\mathbf{k}_\perp = 0$) the Luttinger Hamiltonian is diagonal and the different well subbands are purely light or purely heavy. For small B (also small n and thin QW's) the eigenvectors that appear in Eq. (24) must have only one component different from zero. In this case we can label the state by the well subband index l_i instead of the new quantum number α. For instance, we can label the first heavy-hole subband with $n=0$ as $1_4(0)$. It is

more common to use hh^- instead of 4. Thus, the label would be $hh1(0^-)$. This notation has a clear physical meaning only for small magnetic fields. As an example of the loss of physical meaning we observe (see Fig. 4 of Ref. 17) that the lh1 and hh2 QW subbands are very close to each other in a 100-Å GaAs/AlAs QW and there is an anticrossing around $B = 10$ T, with the paradox that a pure light level at $B = 15$ T would be labeled $hh2(3^+)$.

Figure 2 shows the Raman efficiency as a function of laser energy for $B = 0$ and $d = 100$ Å for the $\bar{z}(\sigma^+,\sigma^+)z$ scattering configuration. The other configuration yields a similar profile although for the other spin components. Figure 2 clearly depicts the difference in the intensity between the heavy and light contributions to the Raman profile resulting mainly from the closeness of the electron and light-hole masses. The overlap integrals $F_{l',l}$ subtracted in Eq. (20) are nearly equal, giving a small contribution to the Raman-scattering efficiency. The $e1$-hh1 outgoing resonance is larger than the incoming one because when the scattered light resonates with the $e1$-hh1 electronic transition the laser light is close to the hh3 level. The same fact makes the $e1$-hh3 incoming transition larger than the outgoing one. The $e1$-hh2 resonance is forbidden by parity.

In Fig. 3 we represent the calculated Raman efficiency as a function of the laser energy for $B = 10$ T in a QW of thickness 100 Å for both scattering configurations $\bar{z}(\sigma^+,\sigma^+)z$ (a) and $\bar{z}(\sigma^-,\sigma^-)z$ (b). According to Eq. (19) for $\bar{z}(\sigma^+,\sigma^+)z$ the resonances are either incoming or outgoing and involve the $v_{lh}^- \rightarrow v_{lh}^-$ or $v_{hh}^- \rightarrow v_{hh}^-$ matrix elements of the electron-phonon interaction. The number of possible transitions is notably reduced by these selection rules. Outgoing transitions are larger than incoming ones due, as in the $B = 0$ case, to the energy denominators. The light and heavy components of the Landau levels make new resonances possible as compared with the parabolic approximation [Fig. 3(b)]. This is the case for the lh1↑ $N = 0(3^-)$(in) and (out) resonances in which the transitions takes place via the $+\frac{3}{2}$ (i.e., spin up) light-hole band (with weights 0.32 and 0.54, respectively).

In Fig. 4 we show the Raman efficiency as a function of magnetic field for $\bar{z}(\sigma^-,\sigma^-)z$ (solid line) and $\bar{z}(\sigma^+,\sigma^+)z$ (dashed line) configurations. The laser energy is so that the transition $e1$-lh1 (1^-) remains outgoing resonant. The first peak around 5 T (solid line) appears when the $e1$-lh1 (2^-) transition crosses the $e1$-lh1 (1^-) transition. The second peak is due to the virtual transition $e1$-hh3 $(0^-) \rightarrow e1$-hh1 (0^-) and it appears because the different slope with respect to the transition that the laser is following makes the product of energy denominators a minimum. The dashed line shows that no resonances show up in the other scattering configuration. Figure 4(b) displays the experimental data (Ref. 7) supposedly obtained in the $\bar{z}(\sigma^+,\sigma^+)z$ scattering configuration. If the configuration of these measurements were the opposite of the nominal one (as a result of an experimental error), the first observed peak would be qualitatively ex-

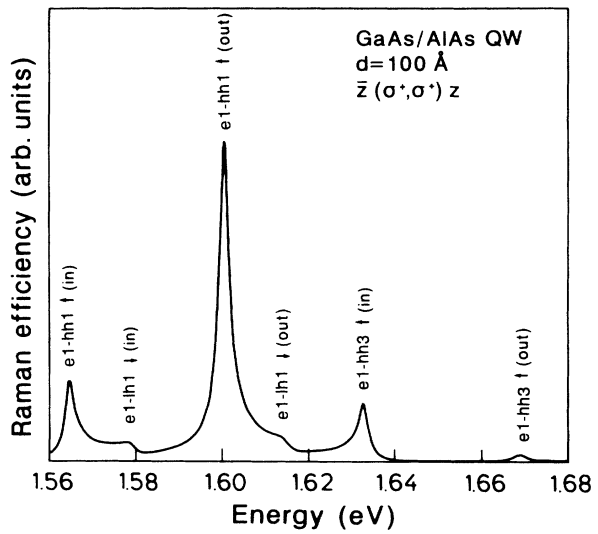

FIG. 2. Calculated Raman-scattering efficiency, according to the scattering amplitude given by Eq. (26), for a GaAs/AlAs QW with $d = 100$ Å and $\hbar\omega_{LO} = 36$ meV at $B = 0$ in the $\bar{z}(\sigma^+,\sigma^+)z$ scattering configuration.

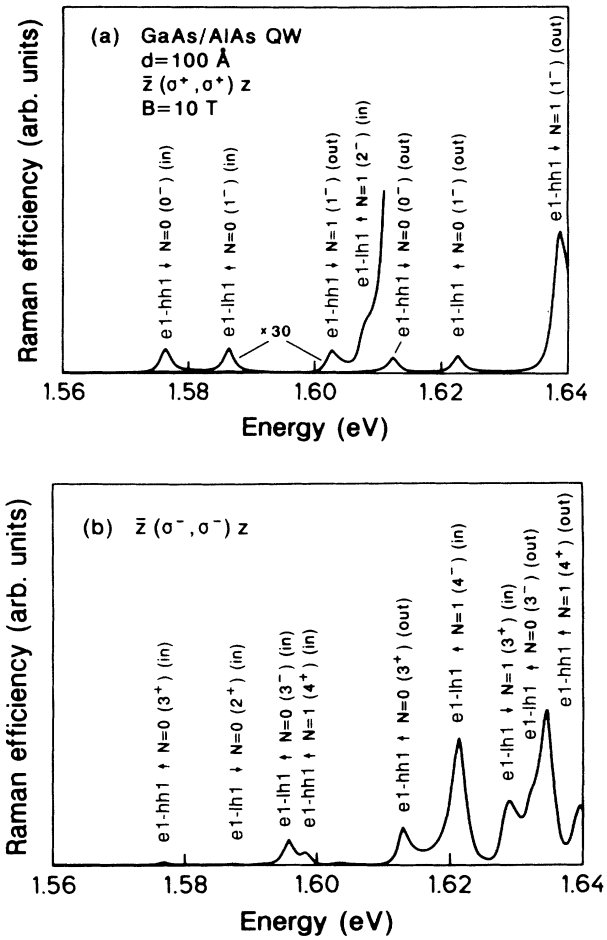

FIG. 3. Magneto-Raman-scattering efficiency for a GaAs/AlAs QW with $d = 100$ Å and $\hbar\omega_{LO} = 36$ meV at $B = 10$ T for both $\bar{z}(\sigma^+,\sigma^+)z$ (a) and $\bar{z}(\sigma^-,\sigma^-)z$ (b) scattering configurations.

plained if we correct for excitonic effects taking a smaller binding energy for upper levels. After this correction, the theoretical peak moves to higher values of magnetic field. The same arguments shift the second theoretical peak to the left.

Figure 5 shows the calculated scattering efficiency as a function of laser energy for a well width of 25 Å. Since this well is very narrow, the different confined phonon modes can be resolved. The difference in intensity between the $p = 2$ and 4 modes is rather large, but it saturates quickly for larger p's.

As can be seen, only even phonon modes are excited. This is due to the fact that in the present analysis we have assumed the same effective-mass Hamiltonian for the diamond and zinc-blende lattices, which means neglecting the very small linear terms which are odd under inversion in the zinc-blende structure. Then, the eigenstates of the Hamiltonian have a definite parity since we operate only with envelope functions, i.e., we neglect the asymmetry of the periodic part of the Bloch functions.

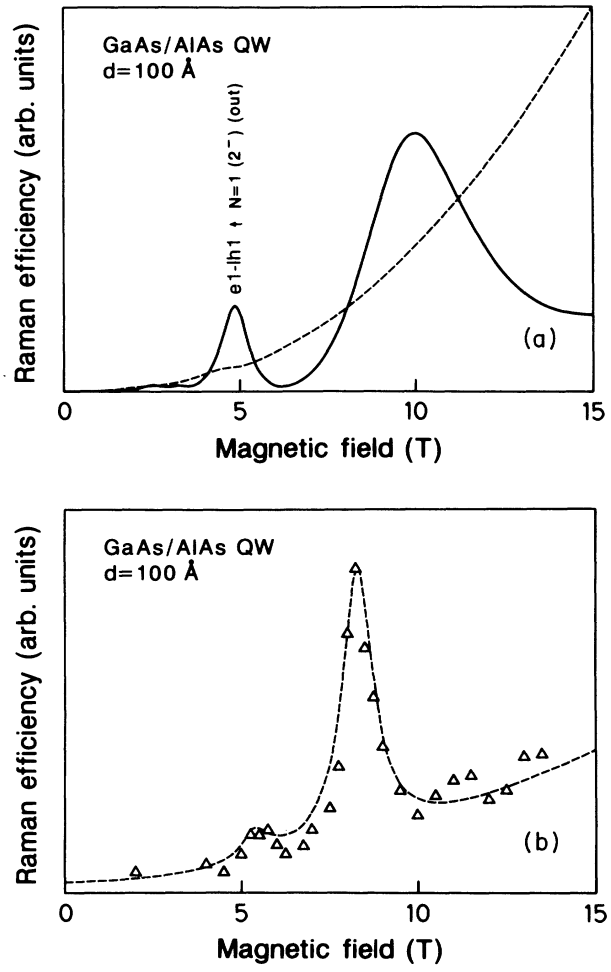

FIG. 4. (a) Raman intensity as a function of the magnetic field for a 100-Å GaAs/AlAs QW calculated for $\bar{z}(\sigma^-,\sigma^-)z$ (solid line) and $\bar{z}(\sigma^+,\sigma^+)z$ (dashed line) configurations with Eq. (26). The curve has been obtained for ω_L following the outgoing transition $e1$-lh1 (1^-). (b) Experimental data points (Ref. 7); the dashed line is a guide to the eye.

IV. CONCLUSIONS

We have developed a theory for the Fröhlich-interaction-induced one-phonon Raman scattering in quantum wells in the presence of high magnetic fields assuming uncorrelated electron-hole pairs. This theory takes into account the confinement of the phonons by the quantum-well potential. The mixing of the valence bands has been treated with a 4×4 Luttinger Hamiltonian. We have shown that only even phonons can be excited due to the parity of the envelope functions involved.

The Fröhlich interaction is allowed for the $\bar{z}(\sigma^\pm,\sigma^\pm)z$ configurations and forbidden in the $\bar{z}(\sigma^\pm,\sigma^\mp)z$ configurations even when the mixing of the valence band is considered. The intensity of the Raman efficiency varies as B^2 and increases with decreasing d in a nontrivial way. For narrow quantum wells ($d \lesssim 50$ Å) the different confined phonon modes have to be treated independently. We have calculated the Raman polarizability for a 100-Å GaAs/AlAs QW and compared it with recent experimental results.

ACKNOWLEDGMENTS

We would like to thank F. Meseguer for helpful discussions and for providing the experimental data prior

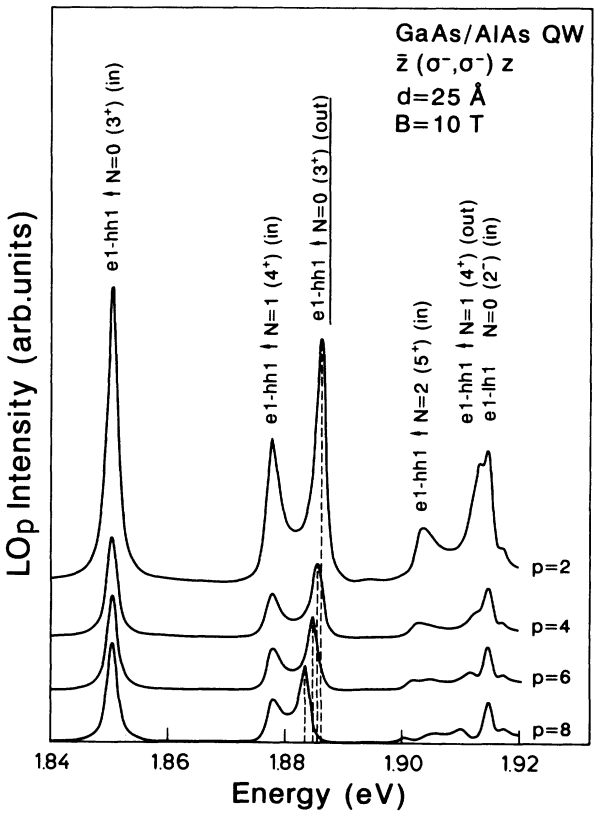

FIG. 5. Raman efficiency for different phonon modes, $p = 2, 4, 6$, and 8. The broken lines represent the shift in outgoing resonances due to the phonon dispersion.

to publication and V.I. Belitskii for a critical reading of the manuscript. One of the authors (A. Cantarero) wishes to acknowledge the Consejo Superior de Investigaciones Científicas and the Deutsche Forschungsgemeinschaft for financial support during his stay at the Max-Planck-Institut.

---

*Permanent address: Departamento de Física Aplicada, Universidad de Valencia, E-46100 Burjasot, Valencia, Spain.

†On leave from Department of Theoretical Physics, Havana University, Havana, Cuba.

[1]G. Ambrazevičius, M. Cardona, and R. Merlin, Phys. Rev. Lett. **59**, 700 (1987).

[2]T. Ruf, A. Cantarero, M. Cardona, J. Schmitz, and U. Rössler, in *Proceedings of the 19th International Conference on the Physics of Semiconductors*, edited by W. Zawadzki (Polish Academy of Sciences, Warsaw, 1988), p. 1473.

[3]T. Ruf, R. T. Phillips, A. Cantarero, G. Ambrazevičius, M. Cardona, J. Schmitz, and U. Rössler, Phys. Rev. B **39**, 13 378 (1989).

[4]T. Ruf and M. Cardona, Phys. Rev. B **41**, 10 747 (1990).

[5]T. Ruf, R.T. Phillips, C. Trallero-Giner, and M. Cardona, Phys. Rev. B **41**, 3039 (1990).

[6]F. Meseguer, F. Calle, C. López, J. M. Calleja, C. Tejedor, K. Ploog, and F. Briones, in *The 5th International Conference on Superlattices and Microstructures, Berlin, 1990* [Superlatt. Microstruct. **10**, 217 (1991)].

[7]F. Calle, J. M. Calleja, F. Meseguer, C. Tejedor, L. Viña, C. López, and K. Ploog, Phys. Rev. B **44**, 1113 (1991).

[8]K. von Klitzing, G. Dorda, and M. Pepper, Phys. Rev. Lett. **45**, 494 (1980).

[9]F. Cerdeira, E. Anastassakis, W. Kauschke, and M. Cardona, Phys. Rev. Lett. **57**, 3209 (1986).

[10]R. C. Miller, A. C. Gossard, G. D. Sonders, V. C. Chang, and N. Schulman, Phys. Rev. B **32**, 8452 (1985).

[11]C. Trallero-Giner, T. Ruf, and M. Cardona, Phys. Rev. B **41**, 3028 (1990).

[12]H. R. Trebin, U. Rössler, and R. Ranvaud, Phys. Rev. B **20**, 686 (1979).

[13]W. Limmer, S. Bauer, H. Leiderer, W. Gebhardt, A. Cantarero, C. Trallero-Giner, and M. Cardona, Phys. Rev. B **45**, 11 709 (1992).

[14]T. Ruf and M. Cardona, Phys. Rev. Lett. **63**, 2288 (1989).

[15]C. Trallero-Giner, F. Iikawa, and M. Cardona, Phys. Rev. B **44**, 12 815 (1991).

[16]Kun Huang, Bang-fen Zhu, and Hui Tang, Phys. Rev. B **41**, 5825 (1990); see also M. Cardona and C. Trallero-Giner, Phys. Rev. B **43**, 9959 (1991).

[17]A. Cros, A. Cantarero, C. Trallero-Giner, and M. Cardona, Phys. Rev. B **45**, 11 395 (1992).

[18]M. Cardona, in *Light Scattering in Solids II*, edited by M. Cardona and G. Güntherodt, Topics in Applied Physics Vol. 50 (Springer, Heidelberg, 1982), p. 19.

[19]A. Cantarero, C. Trallero-Giner, and M. Cardona, Phys. Rev. B **39**, 8388 (1989).

[20]C. Trallero-Giner and F. Comas, Phys. Rev. B **37**, 4583 (1988).

[21]C. Trallero-Giner, F. García Moliner, V. R. Velasco, and M. Cardona, Phys. Rev. B **45**, 11 944 (1992).

[22]The definition differs from Ref. 17 by the factor $\mathbf{e}\cdot\mathbf{p}_{cv}$. Here it has been included in the definition of G_{l_1,l_2}.

[23]See the Bloch wave functions $v(\mathbf{r})$, for instance, in Ref. 11.

[24]J. M. Luttinger, Phys. Rev. **102**, 1030 (1956).

[25]*Heterojunctions and Semiconductor Superlattices*, edited by G. Allan, G. Bastard, N. Boccara, M. Lannoo, and M. Voos (Springer, Heidelberg, 1986).

[26]A. K. Sood, W. Kauschke, J. Menéndez, and M. Cardona, Phys. Rev. B **35**, 2886 (1987).

[27]G. E. W. Bauer and T. Ando, Phys. Rev. B **37**, 3130 (1988).